Atomic layer deposition of environmentally benign $SnTiO_x$ as a potential ferroelectric material

Siliang Chang and Sathees Kannan Selvaraj
Department of Chemical Engineering, University of Illinois at Chicago, Chicago, Illinois 60607

Yoon-Young Choi and Seungbum Hong
Materials Science Division, Argonne National Laboratory, Lemont, Illinois 60439

Serge M. Nakhmanson
Department of Materials Science and Engineering, Institute of Materials Science, University of Connecticut, Storrs, Connecticut 06269

Christos G. Takoudis[a)]
Department of Bioengineering and Chemical Engineering, University of Illinois at Chicago, Chicago, Illinois 60607

(Received 30 August 2015; accepted 30 October 2015; published 12 November 2015)

Inspired by the need to discover environmentally friendly, lead-free ferroelectric materials, here the authors report the atomic layer deposition of tin titanate ($SnTiO_x$) aiming to obtain the theoretically predicted perovskite structure that possesses ferroelectricity. In order to establish the growth conditions and probe the film structure and ferroelectric behavior, the authors grew $SnTiO_x$ films on the commonly used Si(100) substrate. Thin films of $SnTiO_x$ have been successfully grown at a deposition temperature of 200 °C, with a Sn/Ti atomic layer deposition (ALD) cycle ratio of 2:3 and postdeposition heat treatments under different conditions. X-ray photoelectron spectroscopy revealed excellent composition tunability of ALD. X-ray diffraction spectra suggested anatase phase for all films annealed at 650 and 350 °C, with peak positions shifted toward lower 2-theta angles indicating enlarged unit cell volume. The film annealed in O_2 at 350 °C exhibited piezoresponse amplitude and phase hysteresis loops, indicative of the existence of switchable polarization. © *2015 American Vacuum Society*. [http://dx.doi.org/10.1116/1.4935650]

I. INTRODUCTION

Perovskite-based oxides that possess ferroelectric properties, such as $BaTiO_3$ and $PbTiO_3$, have long been the focus of intensive research for decades because of their strong polar, piezoelectric and dielectric properties that make them useful for a wide variety of technological applications. Because of the lead toxicity, a number of computational studies explored the potential replacement of Pb^{2+} by isoelectronic, environmentally benign Sn^{2+}.[1–6] Since the behavior of both ions is governed by the electron lone-pair phenomena, $SnTiO_3$ is supposed to display properties similar to those of its "isoelectronic relative."[4]

A recent theoretical study utilizing first principle calculations has identified perovskite as the most stable polymorph of $SnTiO_3$ (P-SNO).[4] Furthermore, it was shown that P-SNO should have large spontaneous polarization comparable in magnitude or better than that of $PbTiO_3$.[1–5] Yet, the actual synthesis of bulk P-SNO by conventional methods, such as sintering, remains unsuccessful due to the easy disproportionation of Sn^{2+} into Sn^{4+} and Sn metal at high temperatures.[1,3] The loss of the Sn^{2+} oxidation state results in the disappearance of the (stereochemically active) electron lone-pair resulting in a nonpolar material. Nevertheless, thin film deposition techniques provide an alternative route to bypass the limitations imposed by traditional bulk synthesis—e.g., they can stabilize the film structure through misfit strain introduced from the lattice mismatch between the film and the substrate.[7] However, in a recent attempt to synthesize P-SNO via pulsed laser deposition, a growth of nonpolar, ilmenite $SnTiO_x$ thin film on sapphire and perovskite substrates from SnO_2 and TiO_2 targets was reported,[8] suggesting that stoichiometric growth of the $SnTiO_3$ phase exhibiting lone-pair activity was not achieved. This motivated us to conduct a further investigation into the issue of the stabilization of P-SNO in the proper oxidation state using thin film deposition techniques.

Atomic layer deposition (ALD) is a well-established, gas-phase thin film deposition technique that is used to fabricate a variety of thin films that are utilized in many fields such as semiconductor processing, energy harvesting, and catalyst synthesis and design. Its advantages include conformal coating, excellent thickness control, large-area uniformity, and good compositional tunability. ALD can be performed at lower deposition temperatures compared to chemical vapor deposition or pulsed laser deposition, which not only reduces the thermal budget, but also allows the production of films that are unstable at high temperatures. Epitaxial growth of thin films by ALD at low temperature without ultrahigh vacuum has also been reported.[9–12] Indeed, ALD is a suitable technique to tackle the challenge of growing P-SNO.

In this work, we report the preparation of low temperature (200 °C), as-deposited and annealed $SnTiO_x$ thin films on p-type Si substrates using tetrakis(diethylamino)titanium (TDEAT), tin(II)acetylacetonate [$Sn(acac)_2$] and ozone as the reactants. Postdeposition annealing at 350 and 650 °C in N_2, 4% H_2 and O_2 ambient gases was performed to obtain better film

[a)]Electronic mail: takoudis@uic.edu

crystallinity, which is, presumably, also supposed to improve the sample polar properties. X-ray photoelectron spectroscopy (XPS) was used to probe film stoichiometry and ALD compositional tunability. Film structure was studied by x-ray diffraction (XRD), and a pattern corresponding to anatase phase was found for most of the films. Piezoresponse force microscopy (PFM) revealed that the film annealed at 350 °C in O_2 exhibited piezoresponse hysteresis loop, which is an indication of switchable polarization.

II. EXPERIMENT

ALD of tin titanate was performed in our custom-built reactor, using TDEAT and $Sn(acac)_2$ as the metal precursors, and ozone as the oxidant. The reactor is typically operated at ~500 mTorr and has a base pressure of ~20 mTorr. Both precursors were kept in stainless steel bubbler and maintained at 65 and 70 °C, respectively, during deposition. N_2 (99.998%) was used as the carrier gas for both precursors as well as the purging gas to clean the chamber after each reactant's pulse. P-type Si(100) substrates (resistivity: 1–10 Ω·cm, 20 × 20 mm^2) were cleaned according to Radio Corporation of America (RCA) standard cleaning procedure (SC-1), followed by an HF treatment to reduce the native oxide, and finally rinsed by DI water and dried by N_2 blow. Before the codeposition on Si(100), optimization of ALD growth parameters for both oxides were carried out. Precursor pulses for TDEAT and $Sn(acac)_2$ were set to 6 and 8 s, respectively, to saturate the surface.

Thicknesses of the films were measured with a spectroscopic ellipsometer (J.A. Woollam Co., Inc., model M44). Postdeposition annealing was carried out in a preheated quartz horizontal furnace (Lindberg Blue three-zone furnace) under N_2, O_2, and 4% H_2 environment for 5 min at 350 and 650 °C.

Elemental compositions of the films were studied using a high resolution x-ray photoelectron spectrometer (Kratos AXIS-165, Kratoz Analytical, Ltd., United Kingdom) equipped with a monochromatic Al Kα (1486.6 eV) x-ray source operated at 15 kV and 10 mA. Grazing incidence x-ray diffraction (GIXRD) diffractograms were obtained for as-deposited and annealed films using a high resolution x-ray diffractometer (Philips X'pert) configured with a 0.1542 nm x-ray emission line of Cu.

PFM measurements were carried out in a dual AC resonance tracking PFM (DART-PFM) mode (Asylum research, MFP-3D, Santa Barbara, CA, USA) using Pt/Ir coated silicon cantilevers (PPP-EFM, Nanosensors) with tip radius of 30 nm.[13] Vertical piezoresponse hysteresis loops were measured at the contact resonance frequency in DART-PFM mode at three randomly selected points on sample surface. Four measurements were taken at each arbitrary point and averaged to give final results.

III. RESULTS AND DISCUSSION

A. Film growth characteristics

It is crucial to have a sufficient overlap of the constituent binary oxides temperature window before attempting the ternary oxide ALD, in order to easily select the codeposition temperature as well as reproduce the results. Figure 1 shows the temperature dependence of growth rates of both TiO_2 and SnO_x. The region where growth rate is independent of temperature is taken as the temperature window. It can be seen that a wide, overlapping ALD temperature window of 175–275 °C has been obtained. The increased growth rates of both oxides found below the temperature window were attributed to precursors condensation, whereas the decreased TiO_2 growth rate at temperatures above the window resulted from reduced adsorption of precursors onto the substrate surface, and the increased growth rate of SnO_x in this region was likely due to the $Sn(acac)_2$ decomposition. Within this common temperature window suitable for $SnTiO_x$ deposition, the reaction temperatures of each metal oxide as well as the mixed oxide were set to 200 °C.

Figure 2 shows the dependence of $SnTiO_x$, TiO_2, and SnO_x film thicknesses on total number of ALD cycles. Excellent linearity of the curve indicates precise thickness control of the ALD processes that corroborates its self-limiting nature. A TiO_2 film growth rate of 0.05 nm/cycle, and SnO_x film growth rate of 0.1 nm/cycle were found after linear regression analyses (inset). The growth rate of TiO_2 agrees well with that reported earlier by our group using the same precursor but in a different system.[14] SnO_x ALD growth conditions used in this work and its film characterization have been studied by our group and reported elsewhere.[15] Film thicknesses of $SnTiO_x$ (main) also linearly depended on the total number of ALD cycles. It is found that at an ALD cycle ratio (ALDCR) of Sn/Ti = 2:3, the growth rate was 0.07 nm/cycle, indicating a simple linear combination of binary oxide growth rates and a clean codeposition process with no cross-contamination of precursors.

B. Compositional and structural analysis of $SnTiO_x$ thin films

Controlling the composition of each element is another key step in growing targeted ternary oxides. In ALD, this is

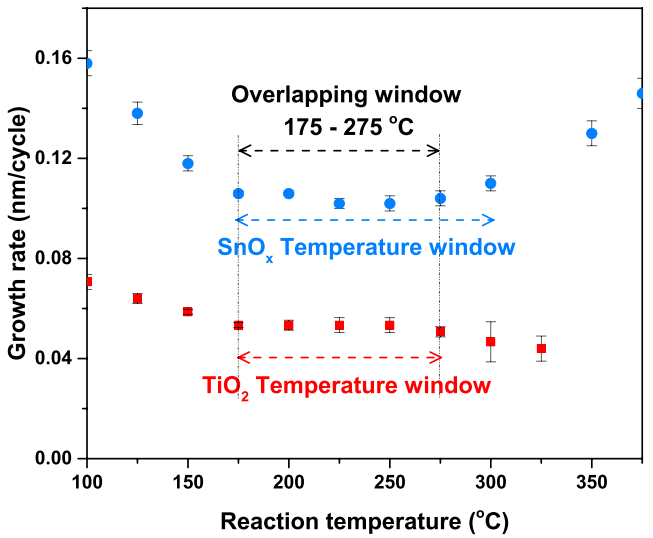

FIG. 1. (Color online) ALD temperature dependence of growth rates of TiO_2 and SnO_x. Error bars indicate film uniformity across the deposition area. Each data point represents the averaged film thicknesses taken at different locations on the sample.

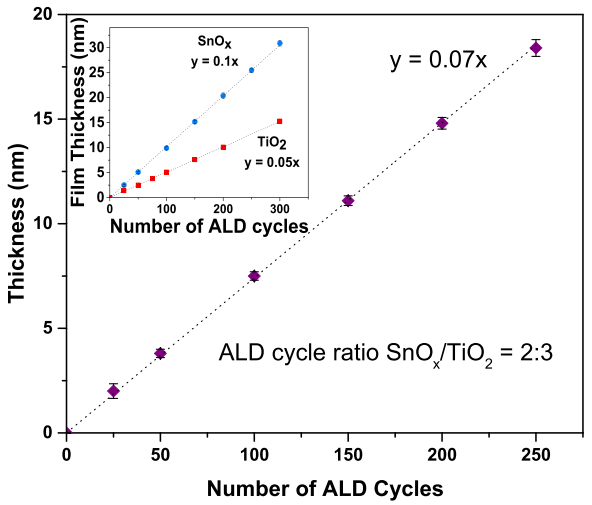

FIG. 2. (Color online) Thicknesses of $SnTiO_x$ thin films with ALDCR of $SnO_x/TiO_2 = 2:3$ dependent on the total number of ALD cycles (main). Film thicknesses of TiO_2 and SnO_x as functions of total ALD cycles are shown in the inset. All ALD reactions were carried out at 200 °C.

achieved by adjusting the ALDCR of metal precursors. A series of seven ALD reactions of $SnTiO_x$ with different ALDCR was performed in order to get the optimal ratio that most likely results in the stoichiometry of $SnTiO_3$. The atomic ratio [Sn/(Sn + Ti)] in the resultant films as a function of normalized ALD cycle ratio was examined by XPS, and shown in Fig. 3. By varying the ALD cycle ratio of SnO_x and TiO_2, Sn content in the films, which spanned from 30% to 80% across different samples, can be effectively controlled. A normalized cycle ratio $[SnO_x/(SnO_x + TiO_2)]$ of 0.4 represents two cycles of SnO_x alternating with three cycles of TiO_2. With this ALDCR, we achieve the atomic ratio of Sn/(Sn + Ti) ~ 0.5, indicating a $SnTiO_x$ stoichiometry. However, excess oxygen was confirmed from XPS elemental

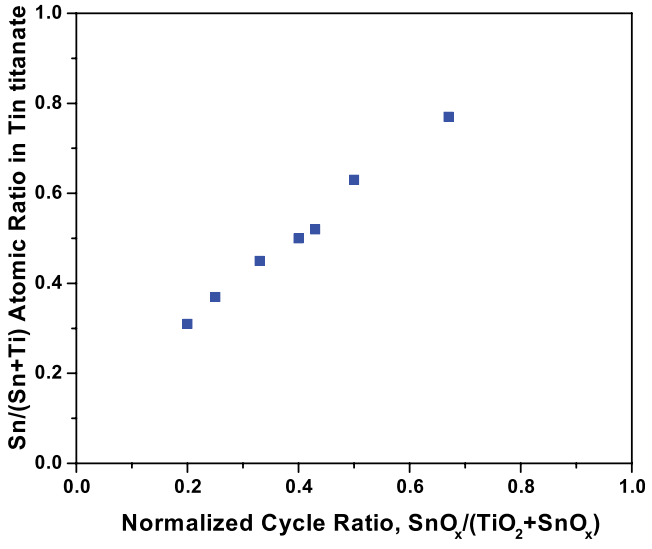

FIG. 3. (Color online) Atomic ratio of Sn/(Sn + Ti) in tin titanate films evaluated using XPS as a function of normalized $SnO_x/(TiO_2 + SnO_x)$ ALD cycle ratio. Other ALD conditions were the same as those in Fig. 2. Sn and Ti atomic percentage used in calculating Sn/(Sn + Ti) were obtained from Sn 3d and Ti 2p scans, respectively.

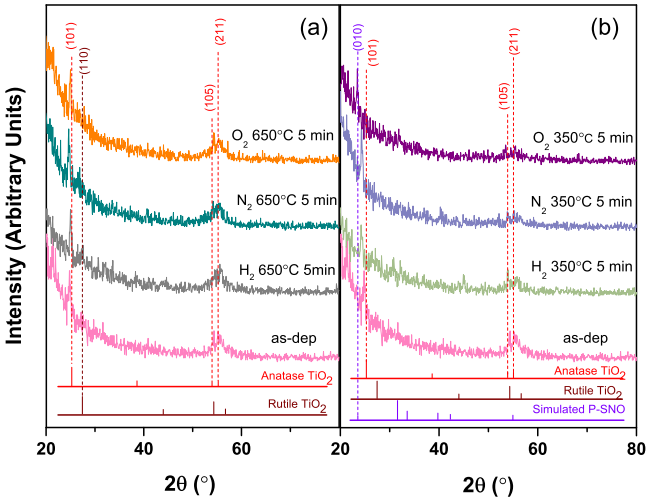

FIG. 4. (Color online) GIXRD patterns of $SnTiO_x$ films annealed at (a) 650 and (b) 350 °C under N_2, 4% H_2 and O_2 environments. Reference diffraction patterns presented at the bottom were obtained from ICDD (PDF card number: anatase, 00-021-1272; rutile, 00-021-1276); P-SNO XRD pattern was simulated based on theoretical studies using CrystalMaker (only major peaks are shown) (Refs. 1–5).

analysis, suggesting an x value slightly greater than three. This can be attributed to the sensitivity of XPS to the surface absorbed, oxygen-containing species, e.g., moisture from ambient exposure, or the use of strong oxidizer such as ozone. About 4 at. % of carbon contamination was detected after 10 min Ar^+ sputtering, which has been reported in thin films grown using β-diketonate precursors.[16]

Due to the metastable nature of Sn^{2+}, the annealing conditions are chosen such that films go through neutral (N_2), oxidizing (O_2), and reducing (4% H_2) heat treatment environments for better comparison. Two annealing temperatures were selected: a lower 350 °C to prevent disproportionation of Sn(II), and 650 °C in the hope of getting better film crystallization. Structures of as-deposited and annealed $SnTiO_x$ films were studied by grazing incidence XRD (GIXRD), as presented in Fig. 4. All films examined were ~40 nm-thick. As-deposited films show diffraction features around 25°, 54°, and 55°, which are assigned to TiO_2 anatase phase with crystal planes of (101), (105), and (211), respectively, signifying film crystallization at deposition temperature (200 °C). Anatase formation at this temperature has been reported in ALD of TiO_2,[17,18] as well as in Sn-doped TiO_2 films grown using spin coating technique.[19] The films annealed at 650 °C [Fig. 4(a)] and 350 °C [Fig. 4(b)] under different ambient gases exhibited similar XRD patterns as those of as-deposited films, suggesting anatase as the major phase after the heat treatments. However, the positions of anatase peaks of all the samples shifted to lower angles without peak broadening, especially for the one annealed in O_2 at 350 °C. This is a clear indication of unit cell enlargement. Since the radius of Sn ion is slightly larger than that of Ti, it is likely that Sn atom gets incorporated into TiO_2 lattice by taking over the position of Ti, thus inducing a lattice distortion which leads to the expansion of the cell volume. As for the film annealed in O_2 at 350 °C that showed the largest peak

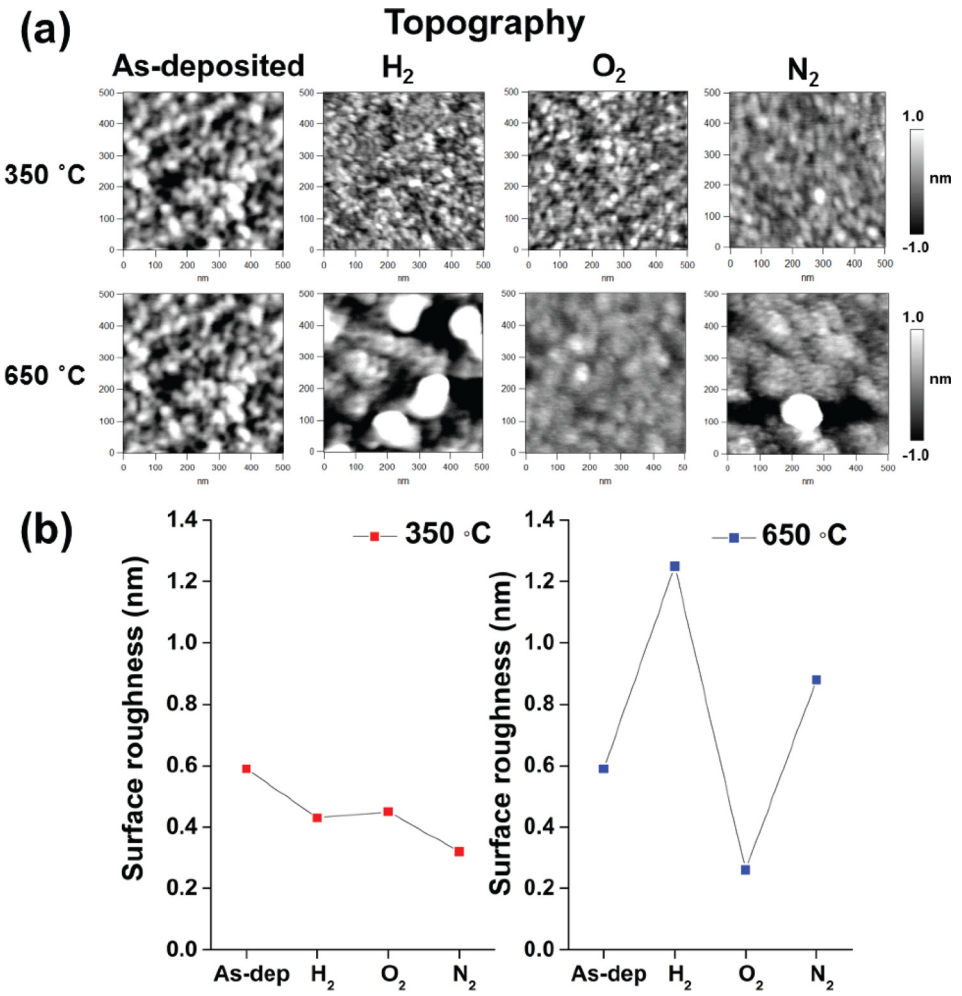

FIG. 5. (Color online) (a) PFM images and (b) surface rms roughness of as-deposited and annealed $SnTiO_x$ films. All measured samples are 40 nm-thick.

shift, its new peak position corresponds to that of (010) orientation of perovskite $SnTiO_3$; however, lack of other evidential peaks from GIXRD pattern prevents drawing definite conclusions on the final structure. Also, the broadened doublet peak at ~54° may indicate the presence of a rutile phase, but its characteristic peak at 27.5° is not observed. Therefore, a further structural investigation, i.e., through TEM, is needed to obtain a better insight into the crystal structure of these thin films.

C. PFM characterization

Surface topography, piezoresponse amplitude and phase images of as-deposited and annealed $SnTiO_x$ films, which were fabricated at various temperatures and gas conditions, were taken on each sample by piezoresponse force microscopy. All films exhibited relatively smooth surfaces with surface rms roughness of below 1.25 nm, as shown in Figs. 5(a) and 5(b). After annealing at higher temperature (650 °C), the particle size increased comparing to the as-deposited films, the surface roughness also increased slightly, which can be explained by the heat-induced particle growth commonly seen in thin films. In order to confirm the presence of piezoelectric and ferroelectric properties in as-deposited and annealed $SnTiO_x$ films, the averaged piezoresponse hysteresis loops were measured from randomly selected regions on each film. Among the samples, only the $SnTiO_x$ film annealed in O_2 at 350 °C showed better-defined piezoresponse amplitude and phase hysteresis loops with coercive voltage of 3.04 V, as shown in Fig. 6. The other films processed under different annealing conditions did not show any meaningful piezoresponse (not shown), ruling out possible

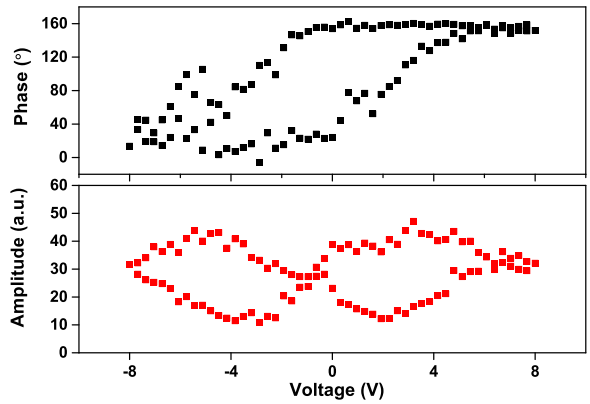

FIG. 6. (Color online) Phase- and amplitude-voltage hysteresis loop of $SnTiO_x$ thin film annealed in O_2 at 350 °C. All measured samples are 40 nm-thick.

ferroelectric properties from PFM data. However, the film annealed in H_2 at 650 °C showed a slanted hysteresis loop (supporting material), which may indicate the existence of leaky ferroelectric phase or hysteretic motion of oxygen vacancies.[20–23]

IV. SUMMARY AND CONCLUSIONS

ALD synthesis of $SnTiO_x$ thin films was successfully carried out on Si substrates by combining two binary oxide ALD processes, with the utilization of tetrakis(diethylamino)titanium and tin(II)acetylacetonate as metal precursors, and ozone as the oxidant. The growth rates of TiO_2 and SnO_x after optimization were found to be 0.05 and 0.1 nm/cycle, respectively. A wide overlapping ALD temperature window of constant growth rates ranging from 175 to 275 °C was obtained. $Sn/(Sn + Ti)$ atomic ratio in $SnTiO_x$ films increased monotonically with increasing normalized $SnO_x/(TiO_2 + SnO_x)$ ALD cycle ratio, indicating the effective composition tunability of the ALD process. Excess oxygen was found by XPS, possibly resulting from surface adsorbed moisture. Film crystallization at deposition temperature (200 °C) was confirmed by GIXRD, and anatase was found to be the major phase for all as-deposited and annealed films. Both as-deposited and annealed $SnTiO_x$ films exhibited relatively smooth surfaces with an rms roughness value of 1.25 nm. The $SnTiO_x$ film annealed in O_2 at 350 °C exhibited a piezoresponse hysteresis loop with a coercive voltage of 3.04 V, which indicates the existence of ferroelectric property. Although the atomic-scale nature of the polarization present in this sample is yet unclear, our study suggests that $SnTiO_x$ indeed has the potential as a ferroelectric material, even when grown on a Si substrate (as opposed, e.g., to a perovskite one, such as $SrTiO_3$). With further structural characterizations underway, we believe these findings will provide useful insights into fabricating perovskite $SnTiO_3$ films with good polar and piezoelectric properties, facilitating further research on lead-free ferroelectric materials.

ACKNOWLEDGMENTS

This project was supported by National Science Foundation (CDMR 1309114, CBET 1067424, and EEC 1062943). The GIXRD studies were carried out in the Frederick Seitz Material Research Laboratory Central Facilities, University of Illinois at Urbana-Champaign. The authors would also like to thank Gregory Jursich for many helpful discussions. The work at Argonne (Y.C. and S.H., PFM imaging and hysteresis loop measurement) was supported by U.S. Department of Energy, Office of Basic Energy Sciences, Materials Sciences and Engineering Division.

[1]Y. Konishi *et al.*, Mater. Res. Soc. Symp. Proc. **748**, U3.13.1 (2003).
[2]Y. Uratani, T. Shishidou, and T. Oguchi, Jpn. J. Appl. Phys. **47**, 7735 (2008).
[3]S. F. Matar, I. Baraille, and M. A. Subramanian, Chem. Phys. **355**, 43 (2009).
[4]W. D. Parker, J. M. Rondinelli, and S. M. Nakhmanson, Phys. Rev. B **84**, 245126 (2011).
[5]H. Ye, R. Zhang, D. Wang, Y. Cui, J. Wei, C. Wang, Z. Xu, S. Qu, and X. Wei, Int. J. Mod. Phys. B **27**, 1350144 (2013).
[6]A. I. Lebedev, Phys. Solid State **51**, 362 (2009).
[7]P. A. Salvador, T.-D. Doan, B. Mercey, and B. Raveau, Chem. Mater. **10**, 2592 (1998).
[8]T. Fix, S.-L. Sahonta, V. Garcia, J. L. MacManus-Driscoll, and M. G. Blamire, Cryst. Growth Des. **11**, 1422 (2011).
[9]D. H. Kim, J.-H. Kwon, M. Kim, and S.-H. Hong, J. Cryst. Growth **322**, 33 (2011).
[10]S. Särkijärvi, S. Sintonen, F. Tuomisto, M. Bosund, S. Suihkonen, and H. Lipsanen, J. Cryst. Growth **398**, 18 (2014).
[11]H. Wang, S. Xu, and R. G. Gordon, Electrochem. Solid-State Lett. **13**, G75 (2010).
[12]M. Coll, J. Gazquez, A. Palau, M. Varela, X. Obradors, and T. Puig, Chem. Mater. **24**, 3732 (2012).
[13]Y. Choi *et al.*, ACS Nano **9**, 1809 (2015).
[14]R. Xu and C. G. Takoudis, ECS J. Solid State Sci. Technol. **1**, N107 (2012).
[15]S. K. Selvaraj, A. Feinerman, and C. G. Takoudis, J. Vac. Sci. Technol., A **32**, 01A112 (2014).
[16]R. L. Puurunen, J. Appl. Phys. **97**, 121301 (2005).
[17]G. Luka, B. S. Witkowski, L. Wachnicki, M. Andrzejczuk, M. Lewandowska, and M. Godlewski, CrystEngComm **15**, 9949 (2013).
[18]M. Reiners, K. Xu, N. Aslam, A. Devi, R. Waser, and S. Hoffmann-Eifert, Chem. Mater. **25**, 2934 (2013).
[19]E. Arpac, F. Sayilkan, M. Asiltürk, P. Tatar, N. Kiraz, and H. Sayilkan, J. Hazard. Mater. **140**, 69 (2007).
[20]I. K. Yoo, *Nanoscale Phenomena in Ferroelectric Thin Films*, edited by S. Hong (Kluwer Academic, Boston, 2004), Chap. 1.
[21]Y. Kim *et al.*, ACS Nano **5**, 9104 (2011).
[22]Y. Kim, A. N. Morozovska, A. Kumar, S. Jesse, E. A. Eliseev, F. Alibart, D. Strukov, and S. V. Kalinin, ACS Nano **6**, 7026 (2012).
[23]N. Balke, S. Jesse, Q. Li, P. Maksymovych, M. B. Okatan, E. Strelcov, A. Tselev, and S. V. Kalinin, J. Appl. Phys. **118**, 072013 (2015).